where γ is the ratio of specific heats; $\alpha = RT_o/u_o^2$; and $\Gamma' = \Gamma h_{so} e^{-\tau_o}/u_o^2$. This is the modified dispersion relation and provides the relationship between the real K and the complex Ω. The method of solution is to assume K and, then, solve for the complex Ω (3 roots) for each location along the nozzle. This corresponds to applying an infinitesimal disturbance of wavelength $2\pi L/K$ at each location and to examine whether the disturbance will grow ($\Omega_i > 0$) or decay ($\Omega_i < 0$). The locus of $\Omega_i = 0$ defines a line (or lines) of neutral stability.

Results and Discussion

Solutions have been obtained for various nozzle configurations. However, for conciseness, we only present one set of example calculations, namely d = 2 and $A_T/A_i = 0.5$. As shown in Fig. 1, the Mach number distributions for this particular nozzle configuration are plotted as functions of τ_o, the optical depth in the steady-state flowfield. Hence the other flow properties such as ρ, u, and T can be calculated. For a given absorber, one can readily transform these results into the physical space by inverting Eq. (4).

The stability map for $\Gamma = 2$ is presented in Fig. 2. These results are for an absorption coefficient of the form, $\kappa \sim \rho^2 T^{-3/2}$, which corresponds to inverse Bremsstrahlung absorption via electrons. The initial temperature T_i and pressure p_i are assumed to be 5000 K and 5 atm, respectively. The glowing gas is taken to be helium with seeded cesium (mole fraction of .001) and the cesium is assumed to be completely ionized to provide sufficient electrons for absorption by inverse Bremsstrahlung.

As shown in Fig. 2, the wavenumber k is plotted against the axial distance with contours of $\Omega_i = 0$. These contours form the boundary between stable and unstable regions in wavenumber space. At each nozzle location, the shaded zone indicates the range of wavenumbers which results in growing disturbances. The unstable zones are located from $x = 0$ to $x = 10$ cm in the region where the absorption takes place. Therefore, if a disturbance has a wavelength much greater than 10 cm, the absorption will only affect a fraction of the wave, and growth of the entire wave will not be significant. Since $k = 2\pi/\lambda$ where λ is the disturbance wavelength, this implies that only $k \lesssim .6$ cm^{-1} are of interest. Hence, the uppermost unstable zone is the only physically important region. It is now desirable to make this region as small as possible to minimize the possibility of unstable heating in the nozzle. It must be remembered that this analysis will not tell us whether a disturbance, which is initiated and grows in one region, will dampen after it travels to a new location. Nevertheless the analysis serves as an important indicator as to where potential absorption wave phenomena may be initiated.

References

[1] Pirri, A. N. and Weiss, R. F., "Laser Propulsion," AIAA Paper 72-719, Boston, Mass., 1972.

[2] Pirri, A. N., Monsler, M. J., and Nebolsine, P. E., "Propulsion by Absorption of Laser Radiation, AIAA Paper 73-624, Palm Springs, Calif., 1973.

[3] Rom, F. E. and Putre, H. A., "Laser Propulsion," NASA TM-X-2510, April 1972.

[4] Hertzberg, A., Johnston, E. W., and Ahlstrom, H. G., "Photon Generators and Engines for Laser Power Transmission," AIAA Paper 71-106, New York, New York, 1971.

[5] Vincenti, W. G. and Traugott, S. C., "The Coupling of Radiative Transfer and Gas Motion," *Annual Review of Fluid Mechanics,* Vol. 3, 1971, pp. 89-117.

[6] Monsler, M. J., "An Acoustic Instability Driven by Absorption of Radiation in Gases." PhD thesis, M.I.T., Dept. of Aeronautics and Astronautics, Cambridge, Mass., 1969.

[7] Vincenti, W. G. and Kruger, C. H., Jr., *Introduction to Physical Gas Dynamics,* Wiley, New York, 1965, p. 463.

[8] Buonadonna, V. R., Knight, C. R., and Hertzberg, A., "The Laser Heated Wind Tunnel," *AIAA Journal,* Vol. 11, Nov. 1973, pp. 1457-1458.

[9] Shapiro, A.H., *Compressible Fluid Flow,* The Ronald Press Co., New York, Vol. 1, 1953.

On Optimum Design of Prestressed Beam Structures

Lewis P. Felton*

University of California, Los Angeles, Calif.

Introduction

A COMPREHENSIVE nonlinear programming formulation of the optimization problem for multiply loaded indeterminate structures, containing design variables associated with diverse forms of prestressing, previously has been presented.[1] Several optimized trusses were examined, and it was shown, e.g., that prestress resulting from lack of fit (i.e., initial element deformations) provided significant reductions in truss weight and led to an otherwise nonfully stressed truss being fully stressed.

It is the purpose of this Note to demonstrate the possible advantages of similar prestressing in beam-type structures. In particular, prestressing by initial deformations will be illustrated for a class of thin-walled indeterminate structures which has been investigated in recent optimization studies.[2,3] This class of structures is well suited to the present application for several reasons. First, optimized thin-walled structures, which satisfy local buckling criteria, provide rational lower bounds on weight. Second, the design problem has been reduced to a particularly simple form, involving only moments of inertia of the elements and prestressing parameters as design variables, and is devoid of inequality behavioral and side constraints, with the exception of non-negativity requirements for moments of inertia and, possibly, limits on the prestressing variables. Finally, optimized unprestressed structures of this class are inherently fully stressed, although maximum stresses vary from element to element, and the effect of prestress on such structures thus should be of distinct interest.

Analysis of Beam Structures with Initial Deformations

Figure 1a shows a uniform beam element with initial deformations equivalent to a relative slope and displacement between ends, denoted, respectively, by θ_0 and δ_0. The equilibrium equation for such an element may be given as

$$P = K\Delta + P_0 \tag{1}$$

where $\boldsymbol{P}$ is a vector of generalized element end forces of the types shown in Fig. 1b, Δ is a vector of associated generalized end displacements, $\boldsymbol{K}$ is the element stiffness matrix, and $\boldsymbol{P}_0$ is interpreted as a vector of fixed-end forces due to applied loads or thermal or initial effects. For a beam with initial displacements as in Fig. 1a, it may be shown that the fixed-end moments M_{1_0} and M_{2_0} are given, respectively, by

$$M_{1_0} = (2EI/\ell)\,[\theta_0 - (3\delta_0/\ell)] \tag{2a}$$

$$M_{2_0} = (2EI/\ell)\,[2\theta_0 - (3\delta_0\ell)] \tag{2b}$$

where E is Young's modulus and I is moment of inertia. Fixed-end shears V_{1_0} and V_{2_0} follow directly from element equilibrium.

The equilibrium equation for an assemblage of these elements is given by

$$F = ku + \beta^T \bar{P}_0 \tag{3}$$

Received Nov. 12, 1975. This research was supported by AFOSR Grant No. 74-2640A, W. Walker, Program Manager, L. A. Schmit Jr., R. B. Nelson, and L. P. Felton, co-principal investigators.

Index category: Structural Design, Optimal.

*Associate Professor, Mechanics and Structures Department. Associate Fellow AIAA.

Table 1 Design results for optimized beams

		Single-load case (load I $=M_A+M_B$)		Multiple-load case (load I $=M_A$, load II $=M_B$)	
		Unprestressed[3]	Prestressed	Unprestressed[3]	Prestressed
	W, lb	6.8077	6.7487	7.3140	6.7350
Independent variables	I_1, in.^{4}	1.2760	1.2686	1.2610	1.2463
	I_2, in.^{4}	2.8610	2.8675	4.0420	2.9726
	δ_{10}, in.	...	−0.0121	...	−0.1243
	$(\theta_{10})^a$	...	$(0.0003)^a$	...	$(0.0031)^a$
Dependent variables	c_1	4.5822	4.5184	4.4553	4.3371
	c_2	3.4464	3.6278	3.6030	3.8715
	A_1, in.^{2}	0.3138	0.3136	0.3134	0.3131
	A_2, in.^{2}	0.5070	0.4976	0.5922	0.4964
	d_1	6.9323	6.7107	6.4941	6.0951
	d_2	3.3692	3.8841	3.8125	4.6082

^{a} Alternate deformation variable.

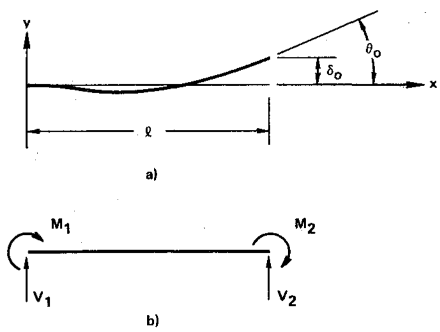

Fig. 1 a) Initially deformed beam element; b) force notation.

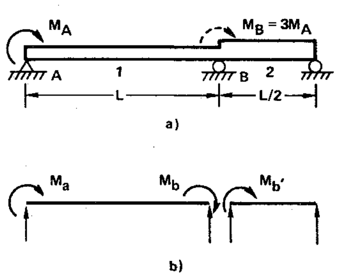

Fig. 2 a) Two-span beam example; b) moment notation.

where F is a vector of forces applied at system displacement coordinates u, k is the system stiffness matrix, β is the compatibility matrix which relates u to element end displacements, and $\bar{P}_0$ is a vector of "assembled" element fixed-end forces. Note that k is related to the assembled element stiffness matrix $\bar{K}$ by $k=\beta^T\bar{K}\beta$.

The quantities θ_0, δ_0 for each element constitute potential design variables, and the analysis of structures prestressed by such initial element deformations thus is given directly in terms of these variables by Eqs. (2) and (3).

Statement of Optimization Problem

The general optimization problem for prestressed structures may be stated in the following form[1]: find the components of a vector of design variables $\tilde{X}^T \equiv [X^T \vdots X_p^T]$ such that

$$g_j(\tilde{X}) \geq 0, \qquad j=1,\dots, J \tag{4}$$

and such that weight $W(\tilde{X})$ is minimized, i.e.,

$$W(\tilde{X}) \to \min \tag{5}$$

where X is a vector of basic variables (as in the unprestressed case), and X_p is a vector of design variables associated with prestress. The inequalities in (4) represent behavioral and/or side constraints. In many cases W may be a function of X only.[1]

Note that, for linear behavior, analysis of the loaded prestressed structure may be achieved by superposition of the response of the unloaded prestressed structure [$F=0$ in Eq. (3)] and that of the loaded unprestressed structure [$\bar{P}_0=0$ in Eq. (3)] . Thus, in addition to the analyses normally required for optimization of an unprestressed structure, optimization of a prestressed structure requires only the analyses of the initial state.

For structures composed of n uniform elements of a class of thin-walled beams with symmetric cross sections defined by four parameters,[3] it has been shown that the basic (unprestressed) optimization problem can be reduced to a form containing only one independent variable per element. That is, find $X^T \equiv [I_1 \dots I_i \dots I_n]$ such that

$$I_i \geq 0, \; i=1,\dots, n \tag{6}$$

and

$$W(X) \propto \sum_{i=1}^{n} c_i(c_i-2)^{-4/9}(c_i+4)^{-5/9} \times (\max_j |M_{ij}|)^{2/9} I_i^{1/3} L_i \to \min \tag{7}$$

where I_i is the moment of inertia of element i, L_i is the specified length of element i, $|M_{ij}|$ denotes the largest magnitude of bending moment in element i under load condition j (and is therefore an implicit function of the I_i), and the c_i are dependent variables given as explicit functions[3] of the quantity $I_i/(\max |M_{ij}|)^{4/3}$. Two additional cross-sectional parameters,[3]† d_i and area A_i, also are given as functions of the I_i and/or c_i.

In view of the preceding, prestressed structures of this class may be optimized by augmenting the vector of design variables such that $\tilde{X}^T \equiv [I_1 \dots I_n \vdots x_1 \dots x_k \dots x_m]$, where x_k represents initial deformations θ_0 and/or δ_0 for various elements. The number of such independent deformation variables m equals the degree of statical indeterminacy of the structure. Except for possible bounds on x_k (note that both positive and negative values are permissible), constraints (6) remain independent of X_p in this case. The objective function of relation (7) is altered only by replacing $\max_j |M_{ij}|$ with

$$\max_j \{\, |M_{i0}|; \; |M_{i0} + M_{ij}| \,\} \tag{8}$$

†Parameters c_i and d_i are denoted by k_{A_i} and k_{I_i}, respectively, in Ref. 3.

Table 2 Bending moments for optimized beams (in.-lb)

		Single-load case (load I $=M_A+M_B$)		Multiple-load case (load I $=M_A$, load II $=M_B$)	
		Unprestressed	Prestressed	Unprestressed	Prestressed
Initial	M_{a0}	...	0	...	0
	M_{b0}	...	707	...	7,202
	$M_{b'0}$	...	−707	...	−7,202
Initial + Load I	M_{a1}	15,000[a]	15,000[a]	15,000[a]	15,000[a]
	M_{b1}	14,338	15,000[a]	6,488	13,402
	$M_{b'1}$	30,662[b]	30,000[b]	−6,488	−13,402
Initial + Load II	M_{a2}	...	...	0	0
	M_{b2}	...	...	6,072	15,000[a]
	$M_{b'2}$	...	...	38,928[b]	30,000[b]

[a] Denotes $\max_j |M_{1j}|$ or $\max_j \{ |M_{10}|; |M_{10}+M_{1j}| \}$.

[b] Denotes $\max_j |M_{2j}|$ or $\max_j \{ |M_{20}|; |M_{20}+M_{2j}| \}$.

where $|M_{i0}|$ is the largest magnitude of initial moment in element i (i.e., in the unloaded prestressed structure), and $|M_{i0}+M_{ij}|$ is now the largest magnitude of moment in element i under load condition j. Thus, the M_{i0} are implicit functions of both X and X_p, whereas the M_{ij} remain implicit functions of X only, as previously.

Examples

Figure 2 shows a two-span beam which has been optimized in previous studies.[2,3] The beam is reconsidered here for optimization, utilizing initial element deformations as a prestressing mechanism. As in previous examples,[3] computations are based on the assumption that the elements have symmetric I-beam cross sections, and on assigned values $M_A=15{,}000$ in.-lb, $L=40$ in., yield stress $=30{,}000$ psi, Young's modulus $=30\times10^6$ psi, material density $=0.3$ lb/in.^{3}, and appropriate flange and web buckling relations.[3]

Results, and comparisons with the previous unprestressed designs, are presented in Table 1. Note that two distinct sets of designs are presented: one set for M_A and M_B applied simultaneously ("single-load" case), and one set for M_A and M_B applied independently ("multiple-load" case). Also note that only one independent initial deformation variable may be chosen in these examples. In order to maintain consistency with Fig. 1 and Eqs. (2), this variable may be taken as either the displacement or slope at the right end of element AB or the displacement at C of element BC. Table 1 shows equivalent optimum values of the first two of these alternate variables. It may be seen that the magnitudes of these variables are relatively small.

For both load cases, the inclusion of prestressing has resulted in weights lower than those of the unprestressed designs. This improvement is particularly significant in the multiple-load case, where the reduction is approximately 8%. This is also noteworthy in view of the fact that the unprestressed structure is inherently fully stressed,[‡] as are all optimum designs composed of this class of elements. It is thus apparent that the prestress leads to alternate, superior, fully stressed designs.

Table 2 illustrates the basis for the weight reductions by displaying the effects of initial deformations on the moment distributions in the optimized beams. Note that, in both load cases, the prestress leads to a reduction in the maximum moment in element 2 and to an equality of moment magnitudes at the ends of element 1. Thus, the moments in element 1, in essence, have been made as uniform as is possible under these load conditions.

It also may be noted that the maximum moments in elements 1 and 2 are now virtually identical in both the single and multiply loaded prestressed beams, which implies that the optimum designs also should be identical. This is confirmed in Table 1, which reflects only minor computational differences in the final designs.

In conclusion, it appears that prestressing by initial deformations is a factor deserving of additional consideration in beam structures as well as in truss structures. Such prestressing can provide significant reductions in weights of optimized structures; alternatively, it also is possible that relatively small but unintentional initial deformations of the type considered herein may degrade the integrity of structures which are optimized without consideration of initial stresses.

[‡] Fully stressed, in this context, is taken to mean that each element is constrained actively under at least one of the load conditions, such that simultaneous flange and web buckling is precluded; consequently, maximum stresses may be different for each element.

References

[1] Hofmeister, L. D. and Felton, L. P., "Prestressing in Structural Synthesis," *AIAA Journal*, Vol. 8, Feb. 1970, pp. 363-364.

[2] Felton, L. P. and Nelson, R. B., "Optimized Components in Frame Synthesis," *AIAA Journal*, Vol. 9, June 1971, pp. 1027-1031.

[3] Nelson, R. B. and Felton, L. P., "Thin-Walled Beams in Frame Synthesis," *AIAA Journal*, Vol. 10, Dec. 1972, pp. 1565-1569.

Some Effects of Combustion on Turbulent Mixing

Louis H. Bangert*
Georgia Institute of Technology, Atlanta, Ga.
and
Daniel I. Sebacher†
NASA Langley Research Center, Hampton, Va.

Introduction

MIXING and reacting compressible and turbulent flows play an important role in supersonic combustion propulsion systems. A question that has arisen in the past is

Received August 19, 1975; revision received November 10, 1975. Sponsored by the National Aeronautics and Space Administration under Grant NGR 11-002-177.

Index categories: Combustion in Gases; Airbreathing Propulsion, Hypersonic.

*Associate Professor, School of Aerospace Engineering. Member AIAA.

†Aerospace Technologist, High-Speed Aeronautics Division, Engine Performance Section.